Cancer Science
Japanese Cancer Association JCA
Open Access

Altered intracellular region of MUC1 and disrupted correlation of polarity-related molecules in breast cancer subtypes

Misato Iizuka,[1] Yoko Nakanishi,[2] Fumi Fuchinoue,[2] Tetsuyo Maeda,[1] Eriko Murakami,[1] Yukari Obana,[2] Katsuhisa Enomoto,[1] Mayumi Tani,[1] Kenichi Sakurai,[1] Sadao Amano[1] and Shinobu Masuda[2]

Departments of [1]Breast and Endocrine Surgery; [2]Pathology, Nihon University School of Medicine, Tokyo, Japan

Key words

Breast cancer, breast cancer subtype, cell polarity, intracellular localization, MUC1

Correspondence

Shinobu Masuda, Department of Pathology, Nihon University School of Medicine, 30-1 Ohyaguchikami-cho, Itabashi-ku, Tokyo 173-8610, Japan.
Tel: +81-3-3972-8111; Fax: +81-3-3972-8163;
E-mail: masuda.shinobu@nihon-u.ac.jp

Funding Information

This work was partially supported by a Grant for "Strategic Research Base Development" Program for Private Universities subsidized by MEXT (2010).

Received April 10, 2014; Revised December 13, 2014; Accepted December 17, 2014

Cancer Sci **106** (2015) 307–314

doi: 10.1111/cas.12596

MUC1 glycoprotein is overexpressed and its intracellular localization altered during breast carcinoma tumorigenesis. The present study aimed to clarify the relationship of cytoplasmic localization of MUC1 with the breast cancer subtype and the correlation of 10 molecules associated with cell polarity in breast cancer subtypes. We immunostained 131 formalin-fixed and paraffin-embedded breast cancer specimens with an anti-MUC1 antibody (MUC1/CORE). For 48 of the 131 tumor specimens, laser-assisted microdissection and real-time quantitative RT-PCR were performed to analyze mRNA levels of MUC1 and 10 molecules, β-catenin, E-cadherin, claudin 3, claudin 4, claudin 7, RhoA, cdc42, Rac1, Par3 and Par6. Localization of MUC1 protein varied among breast cancer subtypes, that is, both the apical domain and cytoplasm in luminal A-like tumors ($P < 0.01$) and both the cytoplasm and cell membrane in luminal B-like (growth factor receptor 2 [HER2]+) tumors ($P < 0.05$), and no expression was found in triple negative tumors ($P < 0.001$). Estrogen receptor (ER)+ breast cancers showed higher *MUC1* mRNA levels than ER− breast cancers ($P < 0.01$). The incidence of mutual correlations of expression levels between two of the 10 molecules (55 combinations) was 54.5% in normal breast tissue and 38.2% in luminal A-like specimens, 16.4% in luminal B-like (HER2+), 3.6% in HER2 and 18.2% in triple negative specimens. In conclusion, each breast cancer subtype has characteristic cytoplasmic localization patterns of MUC1 and different degrees of disrupted correlation of the expression levels between the 10 examined molecules in comparison with normal breast tissue.

Breast cancer is a common cause of death among women worldwide,[1] and its incidence is increasing among Japanese women. Although breast cancer is a heterogeneous disease, gene expression profiling by DNA microarray analysis is furthering our understanding of its biology.[2–4] Intrinsic breast cancer subtypes include luminal A, luminal B, human epidermal growth factor receptor 2 (HER2) overexpressing, basal-like and normal breast-like, which exhibit different prognoses, therapeutic responses and biological behaviors. The St. Gallen International Conference 2013 proposed practical subtypes based on the intrinsic subtypes, and recommended specific treatments.[5] The practical breast cancer subtypes are based on immunohistochemistry results for estrogen receptor (ER), progesterone receptor (PgR), HER2 and Ki-67.[5] Clinicopathologic surrogate definitions exist for luminal A-like, luminal B-like (HER2−), luminal B-like (HER2+), HER2 and triple negative (TN) subtypes. Because treatments are recommended according to subtype, their identification is important.

MUC1 is a highly O-glycosylated, membrane-bound member of the mucin family that is expressed at the apical domain of epithelial cells, including normal breast cells.[6,7] MUC1 has a core protein of 20 amino acid tandem repeats covered by sugar chains.[7–9] The MUC1 core protein includes an extracellular domain, a transmembrane domain and a cytoplasmic tail. During tumorigenic transformation, MUC1 is overexpressed and localized in various intracellular regions.[10,11] Overexpression of MUC1 enables cancer cells to avoid apoptosis,[12,13] and the MUC1 cytoplasmic tail binds to ER-α, β-catenin and p53, which influence tumor growth.[6] From a clinical perspective, a peptide vaccine that targets MUC1 has been developed and is being tested in clinical studies.[14–16] Whether intracellular localization of MUC1 varies according to breast cancer subtype is unclear. Therefore, in this study, we examined the intracellular localization of MUC1 protein in breast cancer subtypes.

The intrinsic subtype is ambiguously related to morphological features such as tubule formation and mucin production. For example, tubular carcinoma and mucinous carcinoma are categorized predominantly into the luminal subtype, while medullary carcinoma belongs mainly to the basal-like subtype.[17] Tubules are an integrated structure based on cell polarity.[18] The tight junction functions as a boundary to distinguish apical and lateral domains, and as a barrier to protect against unselective passage in the intercellular space.[19]

Domains of the plasma membrane are regulated by *Par* and *Crumbs* for the apical domain and *Scribble* for the basolateral domain.[20] In the process to form 3-D tissue from individual cells, the cells alter their actin filament dynamics through activation of the Rho family of GTPases.[18] Thus, cell polarity is organized by molecules regulating junctional structures, domain identity and Rho family GTPases in a coordinated manner. Therefore, we hypothesized that if intracellular localization of MUC1 is altered in breast cancer subtypes, it would be associated with maintenance of cell polarity. To this end, we examined the relationships among representative molecules of junctional structures (β-catenin, E-cadherin, claudin 3, claudin 4 and claudin 7), domain identity (Par3 and Par6), and Rho family members (Cdc42, Rac1 and RhoA) to further understand the altered intracellular localization of MUC1 in breast cancer subtypes.

Table 1. Patients' clinicopathological characteristics

Category	Number of cases
Subtype	
Luminal A	81
Luminal B (HER2−)	11
Luminal B (HER2+)	12
HER2 (non-luminal)	9
Triple negative (ductal)	18
Histology	
Papillotubular	59
Scirrhous	35
Solid tubular	9
Mucinous	6
Noninvasive	6
Mixed type	3
Apocrine	3
Invasive lobular	1
Others	9
Stage	
0	5
I	54
II	77
III	4
IV	2
Tumor size (cm)	
≤2	71
2–≤5	54
>5	6
Lymph node status	
Negative	100
Positive	31
Total cases	131

Materials and Methods

Patients. We examined breast cancer specimens from 131 patients who underwent surgery at Nihon University Hospital Division of Breast and Endocrine Surgery between 2005 and 2007 (Table 1). The patients were 40–70 years of age at the time of their surgeries. No patients received pre-surgical treatment. Breast cancer tissues were fixed in formalin, embedded in paraffin and sectioned. All samples were pathologically examined according to the General Rules for Clinical and Pathological Recording of Breast Cancer[21] and the World Health Organization classification system.[22] The specimens included 125 invasive carcinomas and six noninvasive carcinomas. The study protocol was approved by the institutional ethics committee and conformed to the provisions of the Declaration of Helsinki.

Immunohistochemistry. All breast cancers specimens were examined immunohistochemically for ER (clone 1D5, Dako Cytomation, Carpinteria, CA, USA), PgR (clone PgR686, Dako), HER2 (clone SV2-61γ, Nichirei Bioscience, Tokyo, Japan) and Ki-67 (clone MIB-1, Dako) according to the manufacturers' instructions. Thresholds for receptor positivity were ER ≥ 1%, PgR ≥ 20% and Ki-67 ≥ 14%. HER2 staining was evaluated according to the American Society of Clinical Oncology/College of American Pathologists guidelines.[23] Immunohistochemical intrinsic type definitions were luminal A-like: ER+ /PgR+/HER2−/Ki67^{low}; luminal B-like (HER2−): ER^{+}/HER2^{-}/Ki67^{high} and/or PgR$^{-\ or\ low}$; luminal B-like (HER2+): ER^{+}/HER2^{+}/Ki-67^{any}/PgR^{any}; HER2: ER^{-}/PgR^{-}/HER2^{+}; and TN: ER^{-}/PgR^{-}/HER2^{-}.

All samples were immunostained with an anti-MUC1 antibody (MUC1/CORE, clone Ma552, mouse IgG, Leica Biosystems, Newcastle, UK). Immunohistochemical staining was performed as follows. Paraffin-embedded sections (4-μm thick) of breast cancer specimens were dewaxed, subject to heat-induced antigen retrieval at 121°C for 15 min, cooled and then incubated for 5 min in PBS containing 0.1% Triton-X. The sections were stained with the MUC1/CORE primary antibody (1:200) for 30 min and then the simple Stain MAX PO (MULTI) secondary antibody (Nichirei Bioscience, Tokyo,

Table 2. Sequences of primer sets used for real time RT-PCR

Gene	Forward primers	Reverse primers
MUC-1	5′-CTAGCAGTACCGATCGTAGCC-3′	5′-CCACTGCTGGGTTTGTGTAA-3′
β-catenin	5′-TGGATACCTCCCAAGTCCTG-3′	5′-CAGGGAACATAGCAGCTCGT-3′
E-cadherin	5′-GACTCGTAACGACGTTGCAC-3′	5′ -GGTCAGTATCAGCCGCTTTC-3′
Claudin 3	5′ -TGCTCTGCTGCTCGTGTC-3′	5′-GGTGTTGGTGGTGGTGGT-3′
Claudin 4	5′-AGATGGGTGCCTCGCTCTAC-3′	5′-CCAGGGAAGAACAAAGCAGA-3′
Claudin 7	5′-GGGTGGAGGCATAATTTTCA-3′	5′-AGGACAGGAACAGGAGAGCA-3′
RhoA	5′-CGCTTTTGGGTACATGGAGT-3′	5′-CAAGACAAGGCACCCAGATT-3′
Cdc42	5′-CGAGTTCAAGCGATTCTCCT-3′	5′-CGCCCACAACAACACACTTA-3′
Rac1	5′-AACCAATGCATTTCCTGGAG-3′	5′-GGATAGGATAGGGGGCGTAA-3′
Par 3	5′-TGTTCGACGCAGTAGTGACC-3′	5′-CAGCAGTGTTCTGCTTGAGG-3′
Par 6	5′-TCGCTGGAAAGATCAAAACC-3′	5′-TCCATGGATGTCTGCATAGC-3′
GADPH	5′-GGAAGGTGAAAGGTCGGAGTCA-3′	5′-GTCATTGATGGCAACAATATCCACT-3′

Japan) for 30 min. Colorization was performed with PBS containing 3,3′-diaminobenzidine and 0.5% H_2O_2.

Laser assisted microdissection and extraction of total RNA from breast tumor tissues. As previously described, tissues were mounted as 8-μm-thick paraffin sections on film-coated glass slides, dewaxed with xylene and stained with toluidine blue.[24–26] The breast tumor areas were microdissected using a laser-assisted microdissection system (PALM MBIII, Carl Zeiss Microscopy, Munich, Germany). The microdissected tissues were treated with 200 μL denaturing buffer (2% SDS, 0.1 mM EDTA and 10 mM Tris-HCl). The tissues were then incubated at 55°C with proteinase K until digested completely.

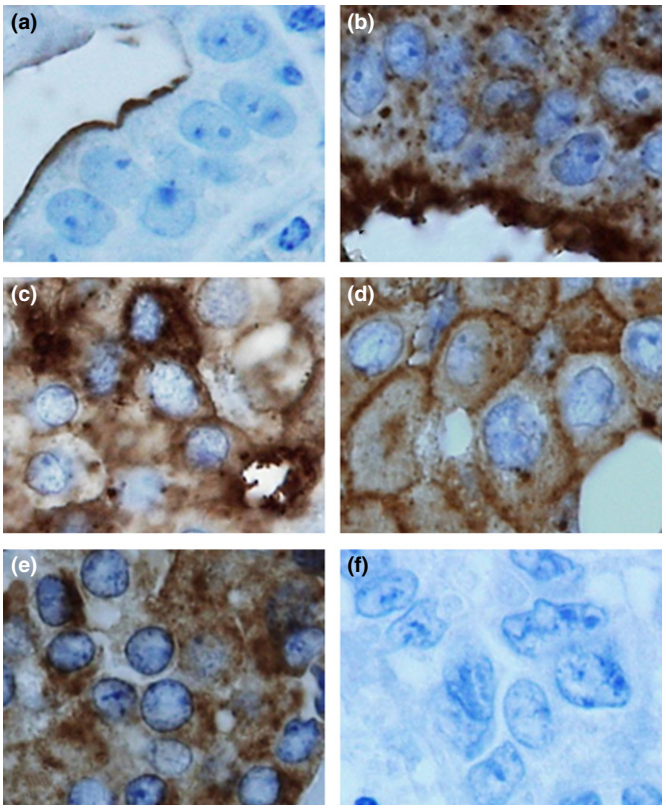

Fig. 1. Intracellular localization pattern of MUC1. MUC1 expression was observed in three locations: the apical domain, cytoplasm and cell membrane. Accordingly, MUC1 localization patterns were classified as: (1) apical only (a); (2) apical + cytoplasm (b); (3) apical + cytoplasm + cell membrane (c); (4) cytoplasm + cell membrane (d); (5) cytoplasm only (e); and (6) negative (f).

Total RNA was purified by adding 20 μL of 2 M sodium acetate (pH 4.0), 220 μL citrate-saturated phenol (pH 4.3) and 60 μL chloroform-isoamyl alcohol, followed by centrifugation for 15 min at 25000g. The upper aqueous layer was transferred into a new tube, mixed with 200 μL isopropanol and 2 μL glycogen, and then incubated at −80°C for at least 30 min. The samples were centrifuged for 30 min at 20000g, washed with

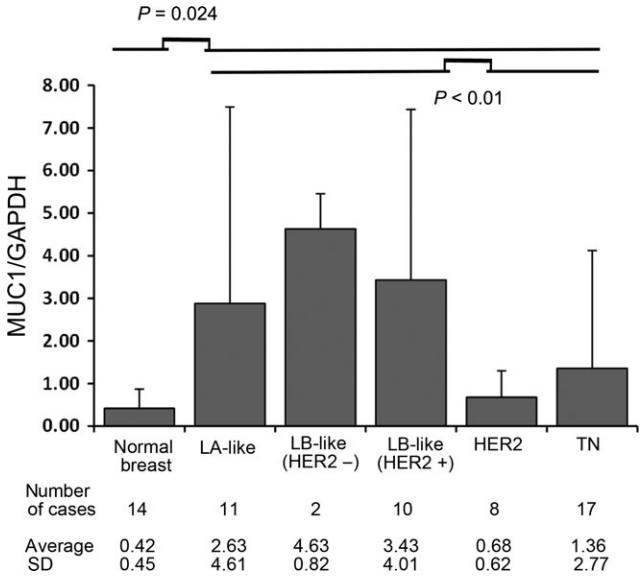

Fig. 2. *MUC1* mRNA levels normalized to *GAPDH* expression in breast cancer subtypes. The number of cases for each breast cancer subtype and the relative *MUC1* mRNA value (mean ± SD) are shown. Expression levels were significantly lower in normal breast tissue than in breast carcinoma ($P = 0.024$). ER+ subtypes showed significantly higher *MUC1* expression than ER− subtypes ($P < 0.01$). ER, estrogen receptor; LA, luminal A-like; LB, luminal B-like; TN, triple negative.

Table 4. Summary of significant patterns of MUC1 intracellular localization by breast cancer subtype as shown by immunohistochemistry

Subtype	MUC1 localization
Luminal A	Apical + cytoplasm**
Luminal B (HER2$^-$)	NS
Luminal B (HER2+)	Cytoplasm + membrane*
HER2	NS
Triple negative	Negative***

*$P < 0.05$; **$P < 0.01$; ***$P < 0.001$. NS, not significant.

Table 3. Intracellular localization patterns for MUC1 in breast cancer subtypes

Pattern	LA		LB (HER2−)		LB (HER2+)		HER2		TN		Total *N*
	n	*P*	*n*	*P*	*n*	*P*	*n*	*P*	*n*	*P*	
(1)	11	0.172	0	0.231	0	0.209	1	0.966	2	0.950	14
(2)	40	0.008*	4	0.773	4	0.598	3	0.652	2	0.006**	53
(3)	1	0.430	0	0.761	0	0.750	0	0.785	0	0.689	1
(4)	5	0.243	2	0.221	3	0.030*	0	0.347	1	0.640	11
(5)	23	0.109	4	0.839	4	0.984	5	0.148	8	0.294	44
(6)	1	0.003**	1	0.666	1	0.735	0	0.428	5	0.001>*	8
Total	81		11		12		9		18		131

(1) Apical-only; (2) apical + cytoplasm; (3) apical + cytoplasm + cell membrane; (4) cytoplasm + cell membrane; (5) cytoplasm-only; and (6) negative. *positive correlation, **negative correlation. LA, luminal A; LB, luminal B; TN, triple negative.

Table 5. Significant correlations among mRNA levels of genes related to cell–cell junction and cell polarity, by breast cancer subtype

Gene 1	Gene 2	Normal breast $n = 15$	LA $n = 11$	LB (HER+) $n = 10$	HER2 $n = 8$	TN $n = 17$
β-*cat*	*E-cad*	$r = 0.89$**	NS	NS	NS	NS
	Cl3	$r = 0.90$**	$r = 0.80$**	NS	NS	$r = 0.81$***
	Cl4	$r = 0.97$**	$r = 0.77$**	NS	NS	NS
	Cdc42	$r = 0.95$**	$r = 0.62$*	NS	NS	NS
	Rac1	$r = 0.95$**	$r = 0.72$*	NS	NS	$r = 0.57$*
	Par3	$r = 0.64$*	$r = 0.66$*	$r = 0.79$**	$r = 0.76$*	$r = 0.94$**
	Par6	$r = 0.90$**	NS	$r = 0.92$***	NS	$r = 0.83$**
E-cad	*Cl3*	$r = 0.82$**	NS	NS	NS	NS
	Cl4	$r = 0.82$**	NS	$r = 0.86$**	NS	NS
	Cdc42	$r = 0.87$**	NS	NS	NS	NS
	Rac1	$r = 0.89$**	NS	$r = 0.79$*	NS	NS
	Par6	$r = 0.88$**	NS	NS	NS	NS
Cl3	*Cl4*	$r = 0.86$**	$r = 0.10$**	NS	NS	NS
	Cl7	$r = 0.86$**	$r = 0.90$***	NS	NS	NS
	Cdc42	$r = 0.94$**	$r = 0.75$**	NS	NS	NS
	Rac1	$r = 0.95$**	$r = 0.95$**	NS	NS	$r = 0.50$*
	Par3	NA	$r = 0.90$***	NS	NS	$r = 0.64$**
	Par6	$r = 0.87$**	NS	NS	NS	$r = 0.59$*
Cl4	*Cl7*	$r = 0.87$**	$r = 0.87$***	NS	NS	NS
	Cdc42	$r = 0.92$**	$r = 0.77$**	NS	NS	NS
	Rac1	$r = 0.91$**	$r = 0.96$**	$r = 0.75$*	NS	NS
	Par3	$r = 0.63$*	$r = 0.92$***	NS	NS	NS
	Par6	$r = 0.82$**	NS	NS	NS	NS
Cl7	*Cdc42*	$r = 0.94$**	$r = 0.64$*	NS	NS	NS
	Rac1	$r = 0.93$**	$r = 0.83$**	NS	NS	NS
	Par3	$r = 0.88$**	$r = 0.75$**	$r = 0.91$***	NS	NS
	Par6	NA	$r = 0.74$**	$r = 0.85$**	NS	NS
Rho A	*Par6*	$r = 0.50$*	NS	NS	NS	NS
Cdc42	*Rac1*	$r = 0.97$**	$r = 0.89$***	NS	$r = 0.79$*	$r = 0.94$**
	Par3	$r = 0.63$*	$r = 0.82$**	$r = 0.67$*	NS	NS
	Par6	$r = 0.94$**	NS	NS	NS	NS
Rac1	*Par3*	NA	$r = 0.93$**	NS	NS	$r = 0.53$*
	Par6	$r = 0.96$**	NS	NS	NS	NS
Par3	*Par6*	NA	NS	$r = 0.87$**	NS	$r = 0.86$**

*$P < 0.05$, **$P < 0.01$, ***$P < 0.001$. β-*cat*, β-catenin; *E-cad*, E-cadherin; *Cl3*, claudin 3; *Cl4*, claudin 4; *Cl7*, claudin 7. LA, luminal A; LB, luminal B; NA, not available; NS, not significant.

70% ethanol, air dried on ice, dissolved in 5–10 μL RNase-free water and then quantified at an optical density of 260 nm using a Nanodrop 1000 (Thermo Fisher Scientific, Waltham, MA, USA). Total RNA samples were stored at −80°C until use. Both genomic DNA elimination and cDNA synthesis were performed with a QuantiTect Reverse Transcription Kit (QIAGEN, Tokyo, Japan) according to the manufacturer's instructions.

Of the 131 specimens examined immunohistochemically, those with a sufficient quantity and quality of extracted mRNA were studied further, which included 48 tumor and 15 normal breast samples.

Real-time quantitative RT-PCR analyses of MUC1 and cell–cell junction and cell polarity-related genes. The mRNA expression levels of *MUC1*, β-*catenin*, *E-cadherin*, *claudins 3*,*4* and *7*, *RhoA*, *Cdc42*, *Rac1*, *Par3*, *Par6* and the internal control *GAPDH* were measured by semi-nested quantitative (snq) RT-PCR.[24] The first RT-PCR was carried out for each target and control cDNA using AmpliTaq Gold 360 Master Mix (Life Technologies Japan, Tokyo, Japan) and the primer sets listed in Table 2. Samples were incubated at 95°C for 10 min and then subjected to 25 cycles of PCR at 94°C for 30 s, 60°C for 30 s and 72°C for 60 s. The first reaction was performed on a conventional PCR machine (PC808, ASTEC, Fukuoka, Japan). One microliter of each resulting product was used as the template in the second snqPCR amplification in an ABI Prism 7000 Sequence Detection System (Life Technologies) using SYBR Green detection chemistry. Briefly, snqPCR amplification was performed in a 20-μL reaction volume containing 900 nmol/L of each primer used in the first RT-PCR and 1× SYBR Green PCR Master Mix (Life Technologies). Reaction mixtures were preheated at 95°C for 10 min, followed by 40 cycles of 95°C for 15 s and 60°C for 1 min. Each relative mRNA value was calculated using the $\Delta\Delta C_t$ method[27] with threshold cycle times for each target mRNA and *GAPDH*.

Analysis of the relationships among molecules related to cell polarity. To examine relationships among molecules related to cell polarity, we estimated correlations between their expression in all 55 combinations. When the numbers of correlated combinations decreased significantly, they were assumed to be deviations from those in normal breast tissue and designated as mild (>50% of normal tissue correlation), moderate (33–50%) or severe (<33%). These deviations were considered to reflect disruptions of cell polarity.

Statistical analysis. Statistical analysis was performed using Stat View for Windows version 5.0. The uniqueness of MUC1

immunohistochemical localization in each subtype was evaluated using the χ^2-test. Correlations between *MUC1* mRNA expression and the breast cancer subtype were analyzed using the Mann–Whitney *U*-test. Deviations in coordinated expression of cell polarity-related molecules from those in normal tissue were estimated using the χ^2-test. The correlation of the expression level of cell polarity-related molecules was analyzed using the Pearson correlation coefficient. Pearson's *r*-value, the strength of the linear relationship between two variables, is shown simply as the "*r*" value, and its statistical significance is shown as *P*-values. $P < 0.05$ was considered to be significant.

Results

Intracellular localization of MUC1 protein and breast cancer subtypes. MUC1/CORE immunoreactivity was positive in 93.9% of samples (123/131) and localized at the apical domain, in the cytoplasm and/or at the cell membrane. The localization of MUC1 protein was classified into six patterns (Fig. 1a–f): (1) apical domain only; (2) at both the apical domain and in the cytoplasm; (3) at the apical domain, in the cytoplasm and at the cell membrane; (4) in the cytoplasm and at the cell membrane; (5) cytoplasm only; and (6) no MUC1 expression detected.

We analyzed the correlations between the cytoplasmic localization patterns of MUC1 protein and each breast cancer subtype (Table 3). In luminal A-like tumors, MUC1 immunoreactivity was localized significantly at the apical domain and in the cytoplasm more frequently than the total of the other five subtypes ($P = 0.008$). In luminal B-like (HER2+) tumors, MUC1 immunoreactivity was localized significantly in the cytoplasm and at the cell membrane more frequently than the total of the other five subtypes ($P = 0.030$). TN tumors were negative for MUC1 more frequently than the total of the other five subtypes ($P = 0.006$). Significant correlations between MUC1 localization and breast cancer subtypes are summarized in Table 4.

Correlation between MUC1 mRNA expression and breast cancer subtypes. *MUC1* mRNA expression levels normalized to *GAPDH* expression were significantly higher in breast carcinoma (relative *MUC1* mRNA value: 2.01 ± 3.62 [mean ± SD]) than in normal breast tissue (relative *MUC1* mRNA value: 0.42 ± 0.45; $P = 0.024$; Fig. 2). In ER+ breast cancers (i.e. luminal A-like and luminal B-like), *MUC1* mRNA expression was significantly higher (relative *MUC1* mRNA value: 3.07 ± 4.46) than in ER− cancers (i.e. HER2 and TN) (relative *MUC1* mRNA value: 1.14 ± 2.38; $P < 0.01$).

Correlation of expression levels of molecules related to cell polarity in breast cancer subtypes. Based on the hypothesis that maintenance of cell polarity affects cytoplasmic localization of MUC1 protein, we analyzed the mRNA expression of 10 molecules related to tight junction (TJ)(claudin 3, 4 and 7), adherens junction (AJ) (β-catenin and E-cadherin), Rho family members (cdc42, Rac1 and RhoA) and domain identity (Par3 and Par6) (Table S1).

We examined correlations between molecules in all 55 combinations, of which 30 of the 55 pairs (54.5%) were correlated significantly and well maintained in normal breast tissues (Table 5), but decreased to 21/55 pairs (38.2%) in luminal A-like (no significant difference compared with 54.5% in normal breast tissue), 9/55 (16.4%) pairs in luminal B-like (HER2+) ($P < 0.001$), 2/55 (3.6%) pairs in HER2 ($P < 0.001$) and 10/55 (18.2%) pairs in TN ($P < 0.001$) breast tumors (Table 5; Fig. 3). Because we only had two luminal B-like (HER2−) cases, this subtype was not examined in the correlation analysis. All subtypes except for luminal A-like had disrupted cell polarity with moderate (TN) or severe (luminal B-like [HER2+], HER2) degrees according to the criteria described in the Materials and Methods. Representative correlations between the molecule pairs are shown in Fig. 4, and their significant correlations are schematically presented in Fig. 5. Expression of AJ-TJ-Rho-Par was positively correlated to normal breast tissue, TJ-Rho-Par were partially correlated to luminal A-like, and only incomplete correlations were found in the other types (Fig. 5).

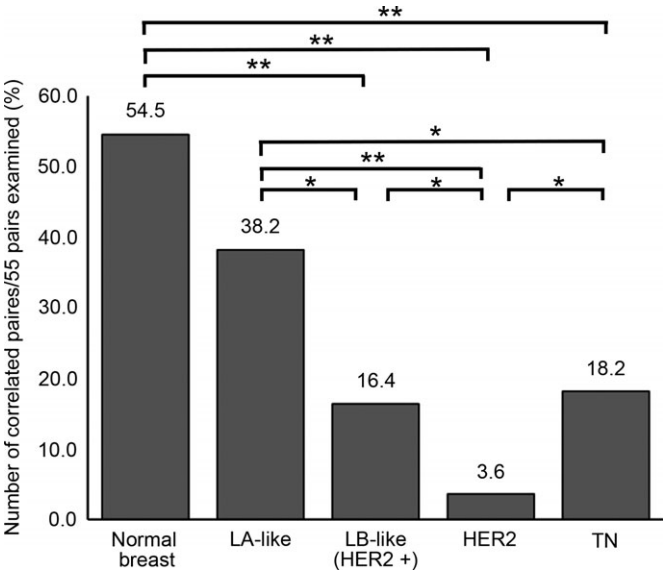

Fig. 3. Degree of correlation between molecules related to cell polarity in breast cancer subtypes. The *y*-axis shows the proportion of correlated pairs (number of correlated combinations among 55 combinations). The deviation from normal breast tissue (54.5%) was analyzed statistically. $^{*}P < 0.05$ and $^{**}P < 0.0001$. LA, luminal A-like; LB, luminal B-like; TN, triple negative.

Discussion

The present study confirmed that *MUC1* mRNA expression was higher in ER+ breast cancers than in ER− breast cancers, as reported previously.[28] Our results also demonstrated that cytoplasmic localization of MUC1 protein varies between breast cancer subtypes, that is, at the apical domain and in the cytoplasm of luminal A-like tumors, in the cytoplasm and at the membrane in luminal B-like (HER2+) tumors, and negative in TN tumors. The recruitment of MUC1 protein at the apical domain, a common pattern in normal breast tissue, was preserved in luminal A-like tumors, but not in other subtypes. It is interesting that another ER+ subtype, luminal B-like (HER2+), lacked the restricted localization at the apical domain. It is well known that carcinoembryonic antigen (CEA) is mainly located at the apical domain of intestinal epithelial cells, but its localization is altered in carcinoma cells. Colorectal cancer cells forming a glandular structure express CEA at the apical domain accompanied by occludin, a protein involved in tight junction, whereas cancer cells arranged in solid nests lacking occludin express CEA diffusely in their cytoplasm.[29] The present study revealed another example of a human cancer presenting an altered distribution of an apical protein.

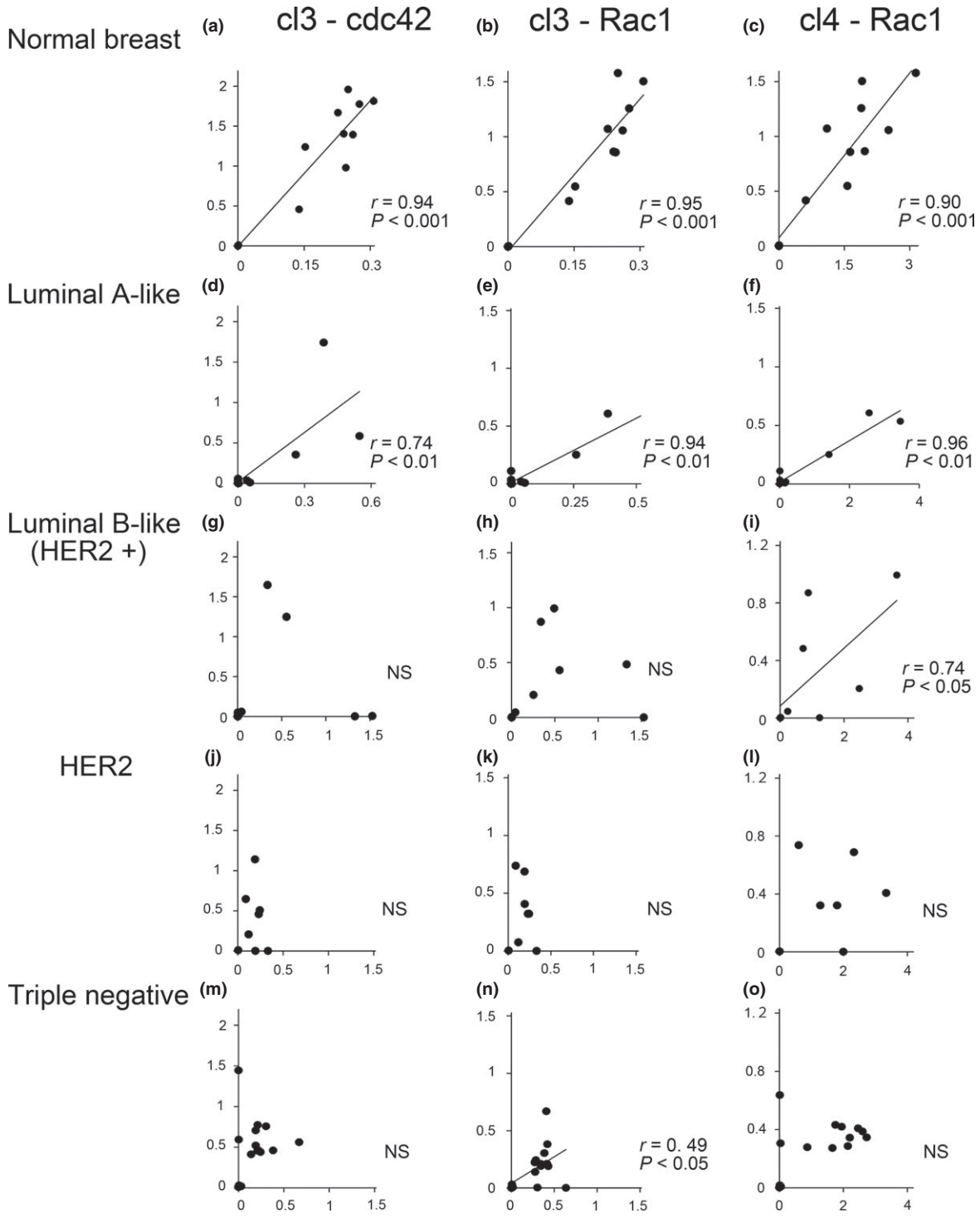

Fig. 4. Correlations between mRNA expression of claudin3-cdc42, claudin3-Rac1, and claudin4-Rac1 in normal breast tissue and breast cancer subtypes. Normal breast (a-c), Luminal A-like (d-f), Luminal B-like (HER2+)(g-i), HER2 (j-l) and Triple negative (m-o) breast cancers were examined for correlations between claudin3-cdc42 (a, d, g, j, m), claudin3-Rac1 (b, e, h, k, n) and claudin4-Rac1 (c, f, i, l, o). Trend lines, correlation coefficients (*r*-values) and statistical significance (*P*-values) are shown. NS; not significant Correlations between cell polarity-related molecules were highly preserved in normal tissue, but less in luminal A-like tumor tissue, and disrupted in other subtypes.

We further demonstrated that whereas the expression levels of molecules involved in tight junction, adherens junction and domain identity, as well as Rho family members were well correlated in normal breast tissue (54.5%), these correlations decreased to 38.2% in luminal A-like, 16.4% in luminal B-like (HER2+), 3.6% in HER2 and 18.2% in TN breast cancer subtypes. By analyzing the results in detail, we uncovered several findings. The correlation between β-catenin and E-cadherin, representative proteins of adherens junction, was preserved in normal breast tissue but lacking in all of the breast cancer subtypes. Furthermore, the correlations among tight junction proteins (claudins 3, 4 and 7) and between TJ-Pars-Rho were preserved

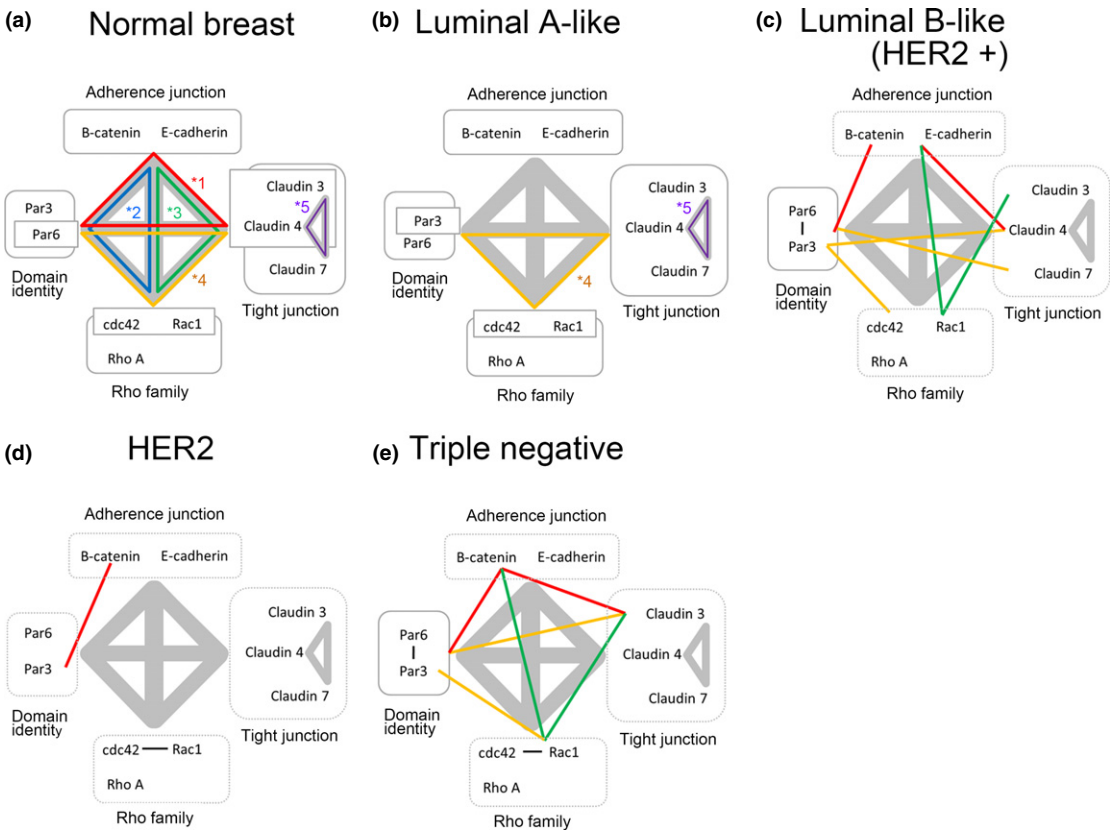

Fig. 5. Schematic summary of correlations between molecules associated with adherens junction (AJ), tight junction (TJ), domain identity (Par) and Rho family members (Rho) in normal breast tissue and breast cancer subtypes. Significant correlations listed in Table 5 are shown as colored solid lines. (a) Normal breast tissue shows significant correlations between AJ-TJ-Par (*1), AJ-Par-Rho (*2), AJ-TJ-Rho (*3), TJ-Par-Rho (*4), and claudins 3, 4 and 7 (*5). (b) The luminal A-like group showed limited correlations among TJ-Par-Rho (*4) and claudins 3, 4 and 7 (*5). Luminal B-like (HER2+) (c), HER2 (d) and triple negative (e) groups showed incomplete correlations among AJ, TJ, Par and Rho.

in normal breast tissue and luminal A-like breast tumors but not in other subtypes. Thus, the present study showed that not only apical localization of MUC1 but also correlations among tight junction proteins (claudins) and TJ-Par-Rho were preserved in luminal A-like breast tumors but not in other subtypes.

Accumulating evidence shows that cells can sense the surrounding environment through receptors (e.g. integrins) and communicate with other cells through junctional structures (adherens and tight junctions). To establish cell polarity, cells have the separated plasma membrane of apical domain, regulated by *Par* (Par3, Par6, aPKC) and *Crumbs* (Crumbs, PALS /Stardust, PATJ/Discs) and basolateral domain regulated by *Scribble* (Scribble, LGL, DLG).[30] In the process to form 3-D tissue from individual cells, the cells alter their actin filament dynamics through activation of the Rho family of GTPases (Cdc42, Rac1 and Rho). The junctional structure and domain identity are also coordinated by protein trafficking systems. Membrane proteins are sorted to apical or basolateral domains from the trans-Golgi network (TGN) or recycling endosomes via precise mechanisms. Sorting mechanisms to the basolateral membrane are well investigated. The basolateral membrane arises from the adaptor protein (AP)-enriched domain, and its sorting is stringently regulated by signals at the cytoplasmic tail, AP and scaffold proteins, including clathrin.[31] In contrast, the apical domain arises from lipid rafts of the TGN, which are enriched with cholesterol, glycosphingolipids and sphingomyelin.[32] Sorting determinants for the apical membrane are diverse and vaguely understood, which include the glycosylphosphatidylinositol anchor,[33] hemagglutinin and neuraminidase,[34] N-glycans[35] and O-glycans,[36] although it has not been fully clarified whether MUC1 is a sorting determinant for the apical membrane. The present study showed that representative molecules contributing to establishment of cell polarity (junctional structures, domain identity and Rho family members), as well as MUC1 were well maintained in normal breast tissue, but disrupted by various degrees in human breast cancer subtypes.

Patients with luminal B-like (HER2+) tumors are expected to benefit from anti-HER2 antibody therapy in addition to hormone therapy. Clinical trials of MUC1 vaccines have been performed for non-small cell lung cancers,[15,16] and these vaccines might be suitable for patients with ER+ breast cancers with high MUC1 expression. The present study raises a further consideration for vaccine therapy, the cytoplasmic localization of MUC1. Whereas the apical domains of epithelial cells in normal breast tissue and luminal A-like tumors usually lay along the lumens of breast tubules, luminal B-like (HER2+) tumors express MUC1 protein at their circumferential cell membrane and may face the fibrovascular stroma. Thus, non-apical localization of MUC1 in luminal B-like (HER2+) tumors, as shown in the present study, may provide an effective means of selecting patients who may benefit from an MUC1 peptide vaccine.

In conclusion, we demonstrated that the cytoplasmic localization of MUC1 protein varies among intrinsic tumor types,

and found different degrees of disrupted correlation of expression levels between the 10 examined molecules in comparison with normal breast tissue.

Acknowledgments

We thank Toshimi Seki, CT (Nihon University Itabashi Hospital, Division of Pathology) for technical support. This work was partially supported by a grant from the "Strategic Research Base Development" program for private universities, subsidized by MEXT (2010).

Disclosure Statement

The authors declare no conflict of interest associated with this manuscript.

References

1 Jemal A, Bray F, Center M, Ferlay J, Ward E, Forman D. Global cancer statistics. *CA Cancer J Clin* 2011; **61**: 69–90.
2 Perou CM, Sorlie T, Eisen MB *et al.* Molecular portraits of human breast tumors. *Nature* 2000; **406**: 747–52.
3 Sörlie T, Perou CM, Tibshirani R *et al.* Gene expression patterns of breast carcinomas distinguish tumor subclasses with clinical implications. *Proc Natl Acad Sci USA* 2001; **98**: 10869–74.
4 Sörlie T, Tibshirani R, Parker J *et al.* Repeated observation of breast tumor subtypes in independent gene expression data sets. *Proc Natl Acad Sci USA* 2003; **100**: 8418–23.
5 Goldhirsch A, Winer EP, Coates AS *et al.* Personalizing the treatment of women with early breast cancer: Highlights of the St Gallen International Expert Consensus on the Primary Therapy of Early Breast Cancer 2013. *Ann Oncol* 2013; **24**: 2206–23.
6 Mukhopadhyay P, Chakraborty S, Ponnusamy MP, Lakshmanan I, Jain M, Batra SK. Mucins in the pathogenesis of breast cancer-implications in diagnosis, prognosis and therapy. *Biochim Biophys Acta* 2011; **1815**: 224–40.
7 Kufe D, Inghirami G, Abe M, Hayes D, Justi-Wheeler H, Schlom J. Differential reactivity of a novel monoclonal antibody (DF3) with human malignant versus benign breast tumors. *Hybridoma* 1984; **3**: 223–32.
8 Gendler SJ, Burchell JM, Duhig T *et al.* Cloning of partial cDNA encoding differentiation and tumor-associated mucin glycoproteins expressed by human mammary epithelium. *Proc Natl Acad Sci USA* 1987; **84**: 6060–4.
9 Gendler S, Taylor-Papadimitriou J, Duhig T, Rothbard J, Burchell J. A highly immunogenic region of a human polymorphic epithelial mucin expressed by carcinomas is made up of tandem repeats. *J Biol Chem* 1988; **263**: 12820–3.
10 van der Vegt B, de Roos MA, Peterse JL *et al.* The expression pattern of MUC1 (EMA) is related to tumor characteristics and clinical outcome of invasive ductal breast carcinoma. *Histopathology* 2007; **51**: 322–35.
11 Yonezawa S, Sato E. Expression of mucin antigens in human cancers and its relationship with malignancy potential. *Pathol Int* 1997; **47**: 813–30.
12 Ren J, Agata D, Kufe D *et al.* Human MUC1 carcinoma-associated protein confers resistance to genotoxic anticancer agents. *Cancer Cell* 2004; **5**: 163–75.
13 Yin L, Kharbanda S, Kufe D. MUC1 oncoprotein blocks hypoxia-inducible factor 1α activation in a survival response to hypoxia. *J Biol Chem* 2007; **282**: 257–66.
14 Rochlitz C, Figlin R, Herrmann R *et al.* Phase I immunotherapy of cancer targeting MUC1 mucin. *J Gene Med* 2003; **8**: 690–9.
15 Ohyanagi F, Horai T, Sekine I *et al.* Safety of BLP25 liposome vaccine (L-BLP25) in Japanese patients with unrespectable stage III NSCLC after primary chemoradiotherapy: Preliminary results from a Phase I/II study. *Jpn J Clin Oncol* 2011; **41**: 718–22.
16 Butts C, Maksymiuk A, Goss G *et al.* Updated survival analysis in patients with stage IIIB or IV non-small–cell lung cancer receiving BLP25 liposome vaccine (L-BLP25): Phase IIB randomized, multicenter, open-label trial. *J Cancer Res Clin Oncol* 2011; **137**: 1337–42.
17 Weigelt B, Horlings HM, Kreike B *et al.* Refinement of breast cancer classification by molecular characterization of histological special types. *J Pathol* 2008; **216**: 141–50.
18 Lie KD, Datta A, Yu W, Brakeman PR *et al.* Rac1 is required for reorientation of polarity and lumen formation through a PI3-kinase-dependent pathway. *Am J Physiol Renal Physiol* 2007; **293**: F1633–40.
19 Tsukita S, Furuse M. Overcoming barriers in the study of tight junction functions: from occluding to claudin. *Genes Cells* 1998; **3**: 569–73.
20 Goldstein B, Macara G. The PAR proteins: fundamental players in animal cell polarization. *Dev Cell* 2007; **13**: 609–22.
21 The Japanese Breast Cancer Society, eds. *General Rules for Clinical and Pathological Recording of Breast Cancer*, 17th edn. Tokyo: Kanehara Shuppan, 2012.
22 Lakhani SR, Ellis IO, Schnitt SJ, Tan PH, de van Vijver MJ, eds. *World Health Organization Classification of Tumours. Pathology and Genetics of Tumours of the Breast*, 4th edn. Lyon: IARC Press, 2012.
23 Wolff AC, Hammond ME, Schwartz JN *et al.* American Society of Clinical Oncology/College of American Pathologists guideline recommendations for human epidermal growth factor receptor 2 testing in breast cancer. *J Clin Oncol* 2007; **25**: 118–45.
24 Nakanishi Y, Shimizu T, Tsujino I *et al.* Semi-nested real-time reverse transcription polymerase chain reaction methods for the successful quantitation of cytokeratin mRNA expression levels for the subtyping of non-small-cell lung carcinoma using paraffin-embedded and microdissected lung biopsy specimens. *Acta Histochem Cytochem* 2013; **46**: 85–96.
25 Mizutani G, Nakanishi Y, Watanabe N *et al.* Expression of somatostatin receptor (SSTR) subtypes (SSTR-1,2A,3,4 and 5) in neuroendocrine tumors using real-time RT-PCR method and immunohistochemistry. *Acta Histochem Cytochem* 2012; **45**: 167–76.
26 Nakanishi Y, Oinuma T, Sano M *et al.* Coexpression of an unusual form of the EWS-WT1 fusion transcript and interleukin 2/15 receptor β mRNA in a desmoplastic small round cell tumour. *J Clin Pathol* 2006; **59**: 1108–10.
27 Macabeo-Ong M, Ginzinger DG, Dekker N *et al.* Effect of duration of fixation on quantitative reverse transcription polymerase chain reaction analysis. *Mod Pathol* 2002; **15**: 979–87.
28 Rakha EA, Boyce RW, Abd El-Rehim D *et al.* Expression of mucins (MUC1, MUC2, MUC3, MUC4, MUC5AC and MUC6) and their prognostic significance in human breast cancer. *Mod Pathol* 2005; **10**: 1295–304.
29 Tobioka H, Isomura H, Kokai Y, Sawada N. Polarized distribution of carcinoembryonic antigen is associated with a tight junction molecule in human colorectal adenocarcinoma. *J Pathol* 2002; **198**: 207–12.
30 Bryant DM, Mostov KE. From cells to organs: Building polarized tissue. *Nat Rev Mol Cell Biol* 2008; **9**: 887–901.
31 Bonifacino JS. Adaptor proteins involved in polarized sorting. *J Cell Biol* 2014; **204**: 7–17.
32 Rodriguez-Boulan E, Kreitzer G, Musch A. Organization of vesicular traffic in epithelia. *Nat Rev Mol Cell Biol* 2005; **6**: 233–47.
33 Brown DA, Rose JK. Sorting of GPI-anchored proteins to glycolipid-enriched membrane subdomains during transport to the apical cell surface. *Cell* 1992; **68**: 533–44.
34 Scheiffele P, Roth MG, Simons K. Interation of influenza virus hemagglutinin with sphingolipid-cholesterol membrane rafts via its transmembrane domain. *EMBO J* 1997; **16**: 5501–8.
35 Fiedler K, Simons K. The role of N-glycans in the secretory pathway. *Cell* 1995; **81**: 309–12.
36 Yeaman C, Le Gall AH, Baldwin AN, Monlauzeur L, Le Bivic A, Rodriguez-Boulan E. The O-glycosylated stalk domain is required for apical sorting of neurotrophin receptors in polarized MDCK cells. *J Cell Biol* 1997; **139**: 929–40.

Supporting Information

Additional supporting information may be found in the online version of this article:

Table S1. mRNA expression of genes related to cell–cell junctions and cell polarity in breast cancer subtypes.